Research Paper

Identification of an energy metabolism-related signature associated with clinical prognosis in diffuse glioma

Zhengui Zhou[1,2,*], Ruoyu Huang[1,3,4,*], Ruichao Chai[1,3,4,*], Xiaohong Zhou[2], Zhiping Hu[2], Wenbiao Wang[2], Baoguo Chen[2], Lintao Deng[2], Yuqing Liu[1,3,4], Fan Wu[1,3,4]

[1]Department of Molecular Neuropathology, Beijing Neurosurgical Institute, Capital Medical University, Beijing 100050, China
[2]Department of Cerebral Surgery, The People's Hospital of Gongan County, Hu Bei, Gongan 434300, China
[3]Department of Neurosurgery, Beijing Tiantan Hospital, Capital Medical University, Beijing 100050, China
[4]Chinese Glioma Genome Atlas Network (CGGA) and Asian Glioma Genome Atlas Network (AGGA), Beijing 100050, China
*Equal contribution

Correspondence to: Fan Wu; **email:** wufan0510284@163.com
Keywords: glioma, energy metabolism, signature, prognosis
Received: July 19, 2018 **Accepted:** October 27, 2018 **Published:** November 8, 2018

ABSTRACT

Now, numerous exciting findings have been yielded in the field of energy metabolism within glioma cells. In addition to aerobic glycolysis, multiple catabolic pathways are employed for energy production. However, the prognostic significance of energy metabolism in glioma remains obscure. Here, we explored the relationship between energy metabolism gene profile and outcome of diffuse glioma patients using The Cancer Genome Altas (TCGA) and Chinese Glioma Genome Altas (CGGA) datasets. Based on the gene expression profile, consensus clustering identified two robust clusters of glioma patients with distinguished prognostic and molecular features. With the Cox proportional hazards model with elastic net penalty, an energy metabolism-related signature was built to evaluate patients' prognosis. Kaplan-Meier analysis found that the acquired signature could differentiate the outcome of low and high-risk groups of patients in both cohorts. Moreover, the signature, significantly associated with the clinical and molecular features, could serve as an independent prognostic factor for glioma patients. Gene Ontology (GO) and Gene Set Enrichment Analysis (GSEA) showed that gene sets correlated with high-risk group were involved in immune and inflammatory response, with the low-risk group were mainly related to glutamate receptor signaling pathway. Our results provided new insight into energy metabolism role in diffuse glioma.

INTRODUCTION

Energy metabolic reprogramming has been a hallmark of cancer cells, which enable tumor cells to generate ATP for maintaining the reduction-oxidation balance and macromolecular biosynthesis—processes that are required for cell growth, proliferation and migration [1]. Many cancers have long been thought to limit their energy metabolism largely to glycolysis producing large amounts of lactate even in the presence of oxygen, a phenomenon known as the Warburg Effect [2]. In comparison to normal cells, tumor cells prefer to incomplete, non-oxidative metabolism of glucose. Until now, it is widely accepted that glucose is the main energy source of cancer cells. However, awareness that the metabolic phenotype of cancer cells is

heterogeneous is growing. Some tumor cells are predominantly glycolytic, whereas others with the given tumor have an oxidative phosphorylation (OXPHOS) metabolic phenotype [3, 4]. Increasing evidences show that there is a metabolic symbiosis between glycolytic and oxidative tumor cells. For example, Lactate and pyruvate generated by glycolysis can be transferred to and used as substrates for tricarboxylic acid (TCA) intermediates and ATP production by the neighbor cancer cells [5]. Similarly, malignant tumor cells also can take up free fatty acids and ketones released by adjacent catabolic cells, which will fuel the mitochondrial OXPHOS for energy production [6, 7]. In addition, it has been reported that glutamine can also be metabolized by TCA cycle to produce energy [8]. Under hypoxic condition, experiments showed that glutamine-driven mitochondrial OXPHOS accounts for most of ATP production [9]. A deeper understanding of Energy metabolism in tumors could offer a vital step forward in the development of new treatments.

Glioma is the most common form of primary malignant brain tumor, with an incidence of 5-6 cases per 100000 persons per year. Glioblastoma (GBM), a highly aggressive tumor, approximately accounts for 55% of glioma with a dismal median survival of 14-16 months [10]. In addition to the diffuse and infiltrative nature, GBM show strong heterogeneity between patients as well as within individual tumor, which leads to the resistance and inevitable recurrence [11, 12]. Despite

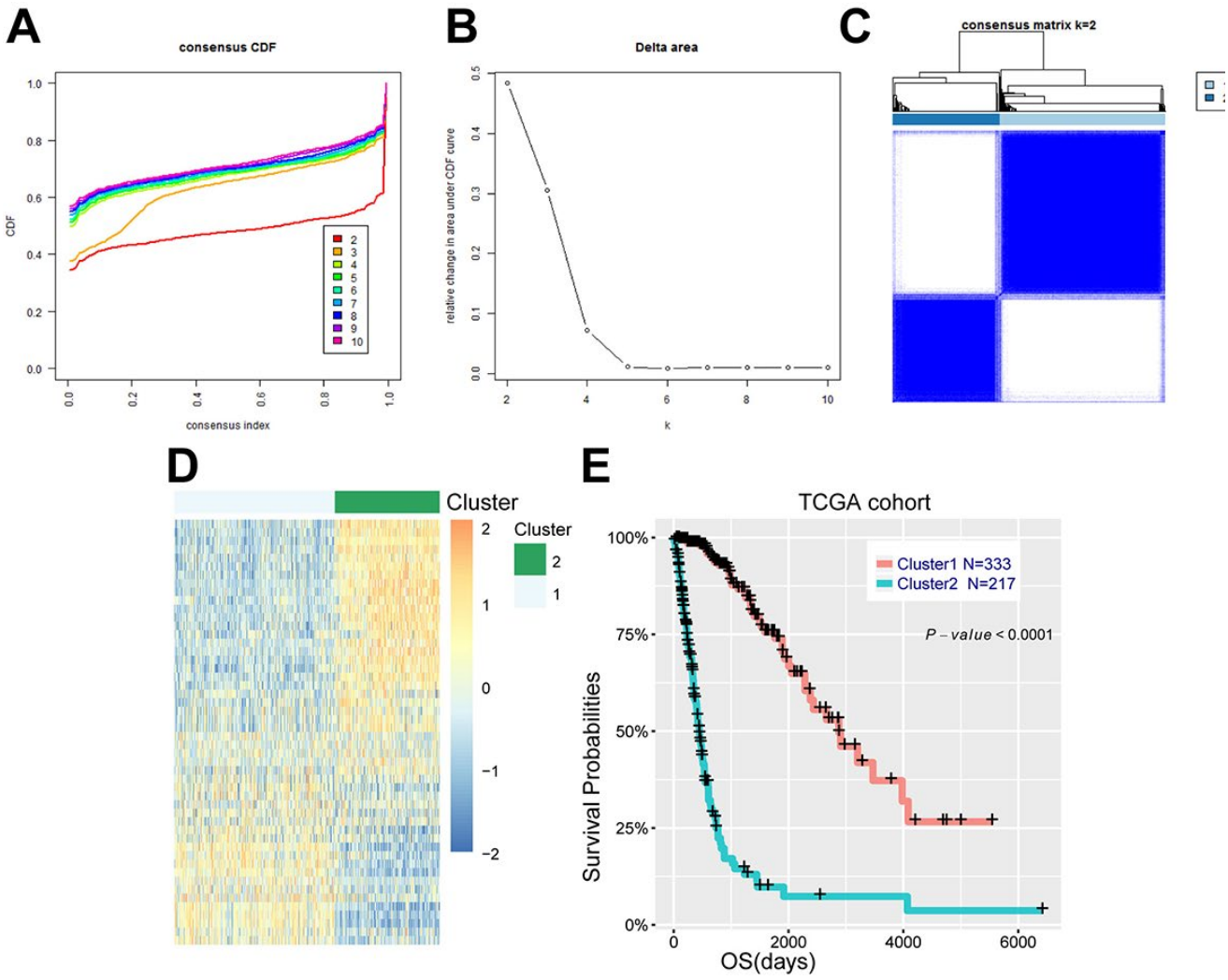

Figure 1. Energy metabolism-related genes could distinguish diffuse glioma patients with different clinical and molecular features. (**A**) Consensus clustering CDF for k = 2 to k = 10. (**B**) Relative change in area under CDF curve for k = 2 to k = 10. (**C**) Consensus clustering matrix of 550 samples from TCGA dataset for k = 2. (**D**) Heat map of two clusters defined by the top 50 variable expression genes. (**E**) survival analysis of patients in cluster 1 and cluster 2.

aggressive treatments, such as surgical resection followed by radiotherapy and chemotherapy, the outcomes of patients with GBM remain very poor [13]. There is an urgent need to find new therapies to improve prognosis for these patients. Accumulating studies have shown that multiple catabolic pathways are involved in energy metabolism of glioma cells [14]. Lin et al reported that primary glioblastoma cells were highly oxidative and largely unaffected by treatment with glycolysis inhibitors, indicating the co-existence of glycolysis and OXPHOS [15]. In particular, glioma stem cells exhibit less glycolytic phenotype compared with their differentiated progeny [16]. Increasingly, recent evidences have shown that glioma cells can also use fatty acids as a substrate for energy production. Inhibition of fatty acid beta-oxidation could reduce the proliferation of glioma cells [17]. However, the local energy metabolic status and its prognostic value in patients with glioma are still remaining to be further elucidated.

In this study, we inquired the energy metabolic profile and its clinical value in patients with diffuse glioma using the TCGA and CGGA RNA sequencing data. Based on the gene expression profile, patients could be classified into two robust groups with significant difference in prognosis and molecular features. Then, we developed an energy metabolism-related signature for assessing the prognosis of glioma patients with TCGA dataset, which was further validated in CGGA dataset. This signature was closely associated with patients' outcome and could serve as an independent pathological factor. To summarize, our results uncovered a strong association between energy metabolism status and clinical prognosis in diffuse glioma.

RESULTS

IDH-wt and IDH-mut LGG show distinct expression profile of energy metabolism genes

To profile the energy metabolism status of glioma, a cohort of 550 patients with RNA sequencing data and clinical information was obtained from the TCGA database. Two energy metabolism-related gene sets were downloaded and integrated into one gene set which contained 587 genes. Within this obtained gene set, 41 genes were involved in carbohydrate metabolism, 73 genes in lipid metabolism and 144 genes in protein metabolism (Supplementary Figure 1A-C). SAM and GO analyses found 25 carbohydrate metabolism genes were differentially expressed between IDH-wt and IDH-mut LGG (Supplementary Figure 1D). Most of the increased genes in IDH-mut LGG were involved in chondroitin sulfate biosynthetic process, while IDH-wt LGG exhibited an enrichment of glycosaminoglycan biosynthetic process (Supplementary Figure 1E). For lipid metabolism, 16 upregulated genes in IDH-mut LGG were mainly involved in fatty acid biosynthetic, while 23 increased genes in IDH-wt LGG were related to bile acid biosynthetic and oxidation-reduction process (Supplementary Figure 1F and G). For protein metabolism, IDH-mut LGG displayed enrichment of translational initiation, whereas IDH-wt LGG exhibited enrichment of protein N-linked glycosylation (Supplementary Figure 1H and I). These results suggested a significant difference of energy metabolism status between IDH-wt and IDH-mut LGG.

Table 1. Characteristics of patients in class 1 and class 2 in TCGA cohort.

Characteristics	n	Class 1	Class 2	*P*-value
Total Cases	550	333	217	
Age				
≤48	287	240	47	**<0.001**
>48	263	93	170	
Gender				
Male	319	185	134	0.321
Female	231	148	83	
Subtype				
Classical	141	6	135	**<0.001**
Mesenchymal	31	1	30	
Proneural	345	299	46	
Neural	33	27	6	
Grade				
II	191	181	10	**<0.001**
III	211	151	60	
IV	148	1	147	
IDH				
Mut	338	319	19	**<0.001**
WT	212	14	198	
MGMT promoter				
Methylated	383	302	81	**<0.001**
Unmethylated	135	31	104	
NA	32	0	32	

IDH = isocitrate dehydrogenase; MGMT = methylguanine methyltransferase.

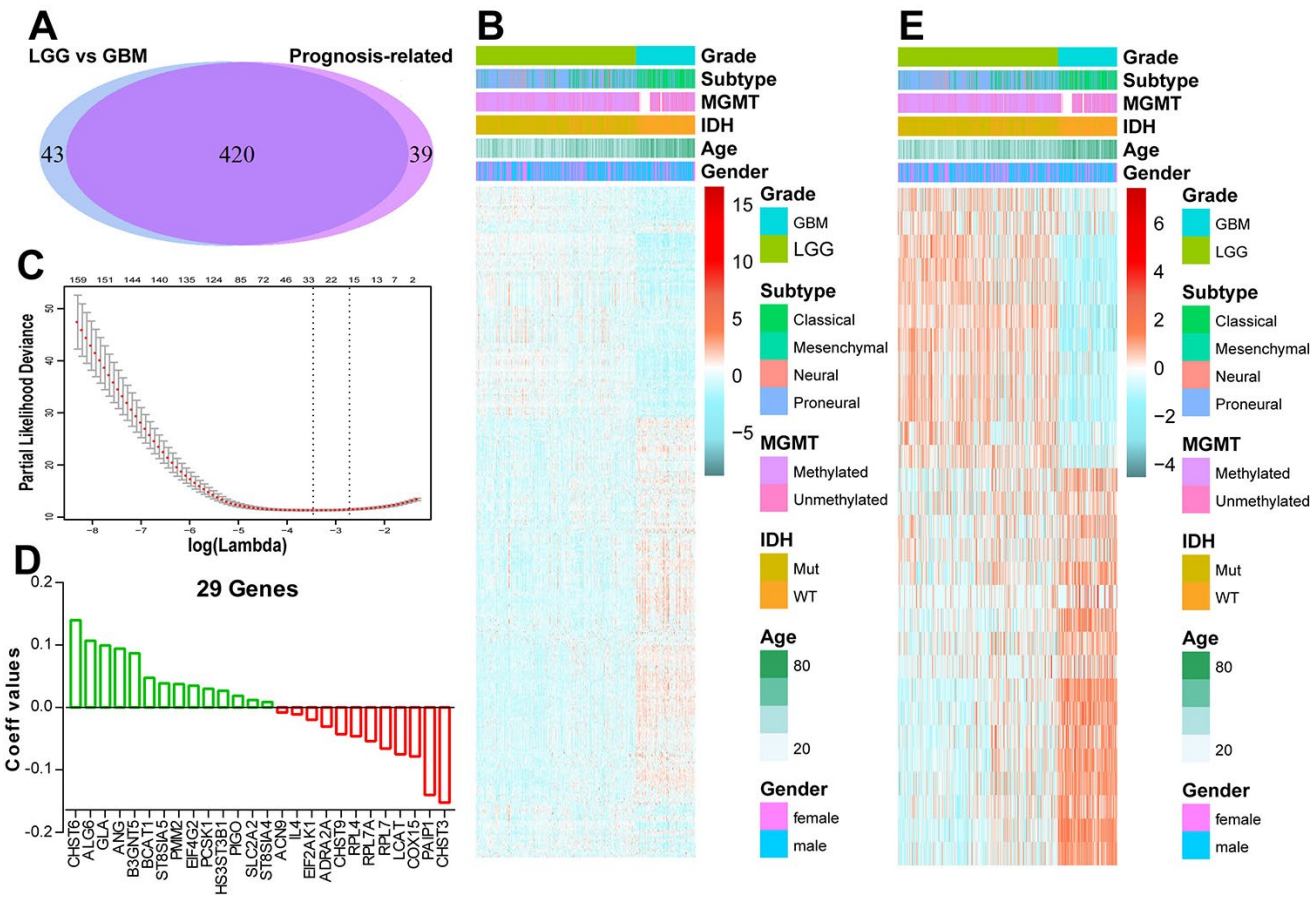

Figure 2. Identification of an energy metabolism-related signature by Cox proportional hazards model in TCGA cohort. (**A**) Venn diagram shows prognosis-related genes which are also differentially expressed between LGG and GBM. (**B**) Heat map of 420 energy metabolism-related genes correlated with patients' OS. (**C**) Cross-validation for tuning parameter selection in the proportional hazards model. (**D**) Coefficient values for each of the 29 selected genes. (**E**) Heatmap of the 29 genes of the signature based on the risk score value.

Identification of an energy metabolism-related prognostic signature in diffuse glioma

We further explored the association between energy metabolism status and outcome of diffuse glioma patients. Consensus clustering found that patients could be classified into two robust groups (Figure 1A-C). Figure 1D showed the heat map of these two clusters defined by the top 50 variable expression genes. Kaplan-Meier analysis revealed that patients in cluster 1 had a significantly longer OS than those in cluster 2 (Figure 1E, $P<0.001$). To further detect the difference between these two clusters of patients, Chi-square test was performed. Patients in cluster 1 were mainly younger, lower grade, proneural or neural subtype, IDH mutational and MGMT promoter methylated ($P<0.001$), while cluster 2 represented older, high grade, classical or mesenchymal subtype, IDH wild type, and MGMT promoter unmethylated ($P<0.001$) (Table 1). Similarly, the CGGA cohort of 309 patients with RNA sequencing data and clinical information was also downloaded and analyzed, and consistent results were observed (Supplementary Figure 2, Supplementary Table 1). These results indicated that expression of energy metabolism-related genes was closely correlated with patients' prognosis and molecular features in diffuse glioma.

Considering the strong link between patients' prognosis and energy metabolism status, we proposed to develop an energy metabolism-related signature for prognosis prediction. SAM analysis found that 463 genes were differentially expressed between LGG and GBM based on the *P* value. Univariate Cox regression analysis revealed 420 out of the differential genes were significantly correlated with patients' OS, as shown in Figure 2A and B. Then, we applied a Cox proportional hazards model for selecting genes with best prognostic value (Figure 2C). A 29-gene signature was identified (Figure 2D and E) and the risk score was calculated

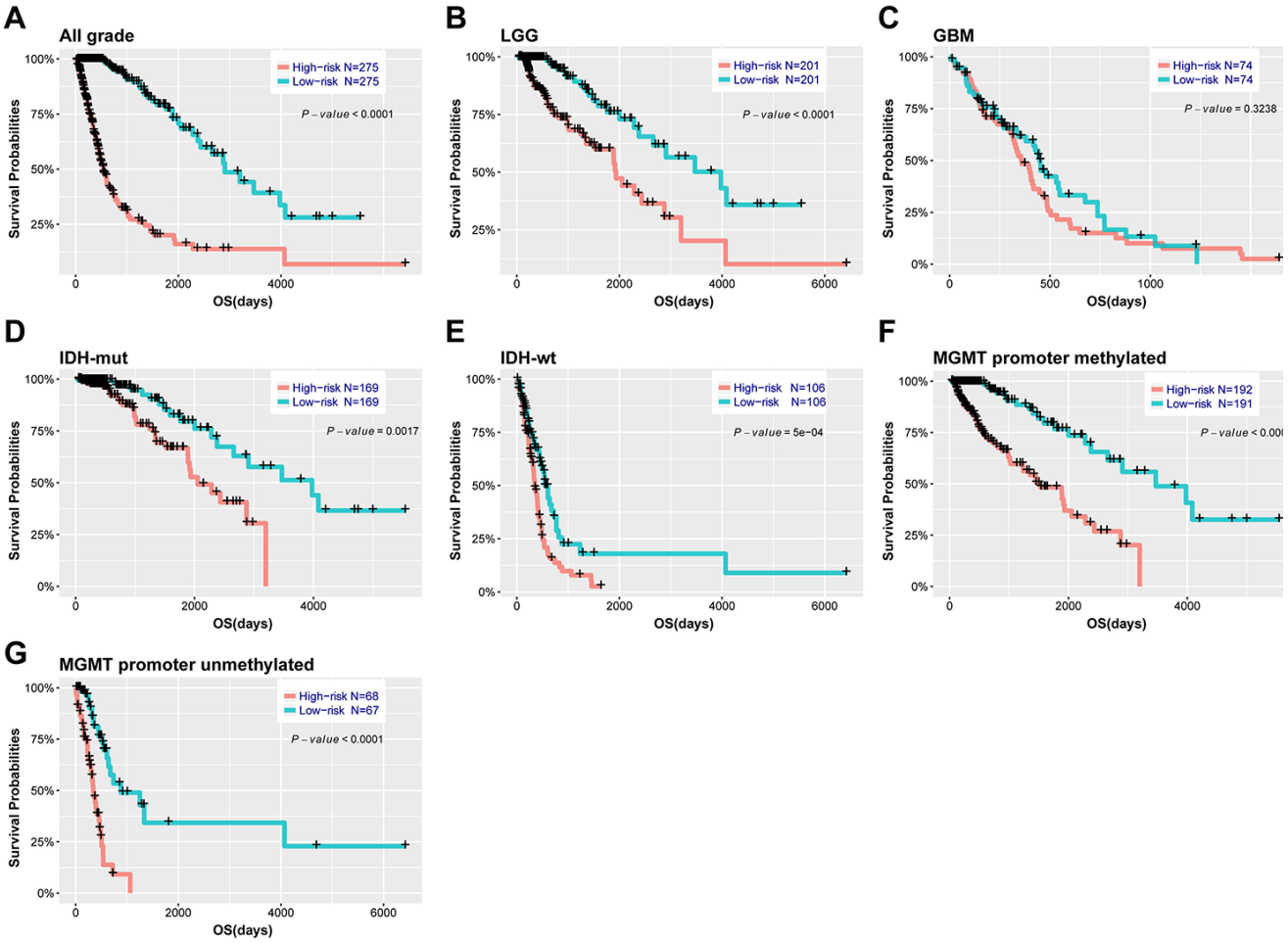

Figure 3. Outcome prediction of the 29-gene signature in stratified patients of TCGA cohort. (**A-G**) survival analysis of the signature in patients stratified by grade, IDH and MGMT promoter status.

with their expression level and regression coefficients. The biological function of these 29 genes was annotated with GO analysis (Supplementary Figure 3). For the CGGA validation set, the risk scores of patients were computed with the same regression coefficients.

29-gene signature shows strong power for prognosis assessment

Based on the median risk score, patients were assigned into high-risk and low-risk groups. Kaplan-Meier analysis showed patients in low-risk group had a significantly longer OS than those in high-risk group (Figure 3A, P<0.001). Then, we further explored the prognostic value of this signature in stratified patients by grade, IDH status, MGMT promoter status. The similar results were observed in most stratified patients expect patients with GBM (Figure 3B-G). Similarly, the prognostic value of this signature was also evaluated in the CGGA validation set. Consensus results were obtained by Kaplan-Meier analysis (Supplementary Figure 4). Further stratified analyses also revealed that high risk score conferred reduced OS in molecular subgroups (LGG IDH-wt, LGG IDH-mut and GBM IDH-mut) in both cohorts (Supplementary Figure 5). Univariate and multivariate Cox regression analysis revealed that this risk score was significantly corelated with patients' OS (95% CI=1.415-2.907, P<0.001), independent of age, gender, grade, subtype, IDH and MGMT promoter status (Table 2). Furthermore, the risk score could also serve as an independent prognostic factor in CGGA cohort (95% CI=1.161-2.086, P=0.003) (Supplementary Table 2).

Using ROC curve, we further evaluated the predictive accuracy by computing AUC (area under the curve) of risk score, age and grade. The AUC of risk score (87.2%) was much higher than that of age (80.1%) and grade (83.0%) (Figure 4A). Moreover, The AUC of risk score (79.1%) was substantially higher in CGGA

Table 2. Univariate and multivariate Cox regression analysis of clinical pathologic features for OS in TCGA cohort.

Characteristics	Univariate analysis			Multivariate analysis		
	HR	95% CI	*P*-value	HR	95% CI	*P*-value
Age	1.076	1.063-1.089	**<0.001**	1.059	1.042-1.076	**<0.001**
Gender	0.957	0.705-1.299	0.779			
Grade	5.285	4.047-6.902	**<0.001**	1.315	0.888-1.946	0.171
Subtype	2.398	2.038-2.822	**<0.001**	0.973	0.754-1.255	0.832
IDH	0.101	0.07-0.144	**<0.001**	1.517	0.568-4.052	0.405
MGMT promoter	0.276	0.196-0.39	**<0.001**	0.812	0.546-1.208	0.305
Risk score	2.434	2.144-2.764	**<0.001**	2.028	1.415-2.907	**<0.001**

HR = hazard ratio; CI = confidence interval; IDH = isocitrate dehydrogenase; MGMT = methylguanine methyltransferase.

validation set (Figure 4B). These data demonstrated the powerful ability of the energy metabolism-related signature for predicting prognosis.

Energy metabolism-related signature is associated with pathologic features in diffuse glioma

We next determined whether the 29-gene signature was related to patients' clinical molecular features. Patients were arrayed based on their risk scores. The signature scores distributed differently in stratified patients, with high level in high grade, classic or mesenchymal, IDH wild type and MGMT unmethylated patients (Figure 5). The statistical difference of these features between high and low-risk groups was evaluated using chi-square test. Except gender, most of features were found different between risk groups (Table 3, $P<0.001$). Additionally, similar results were obtained in CGGA cohort of glioma patients (Supplementary Figure 6, Supplementary Table 3). These findings indicated a significant correlation between energy metabolism signature and pathologic features in diffuse glioma.

Functional annotation of 29-gene signature

We further compared gene expression between the high-risk and low-risk groups. PCA showed that high and low-risk groups of patients tended to distribute in two sides clearly in both TCGA and CGGA cohort (Supplementary Figure 7). Based on the top 2000 genes of differential expression ($P<0.05$, ranked by fold change) identified by SAM, GO analysis revealed that antigen processing and presentation, immune response, inflammatory response and T cell costimulation were significantly enriched in high-risk group, while the low-risk group showed enrichment of translational initiation

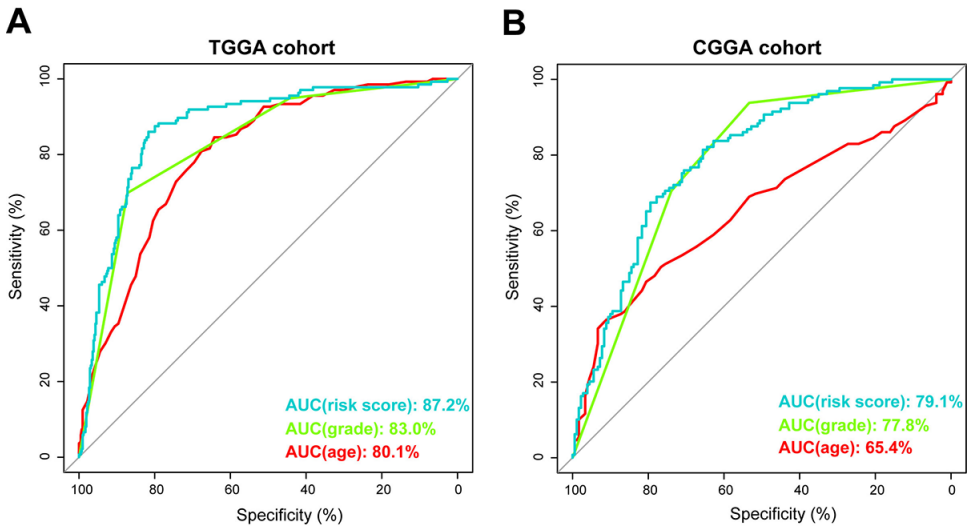

Figure 4. Prognostic power of the identified 29-gene signature in TCGA and CGGA cohorts. (**A**) ROC curve analysis of age, grade and risk score in TCGA cohort. (**B**) ROC curve analysis of age, grade and risk score in CGGA cohort. AUC, area under the curve.

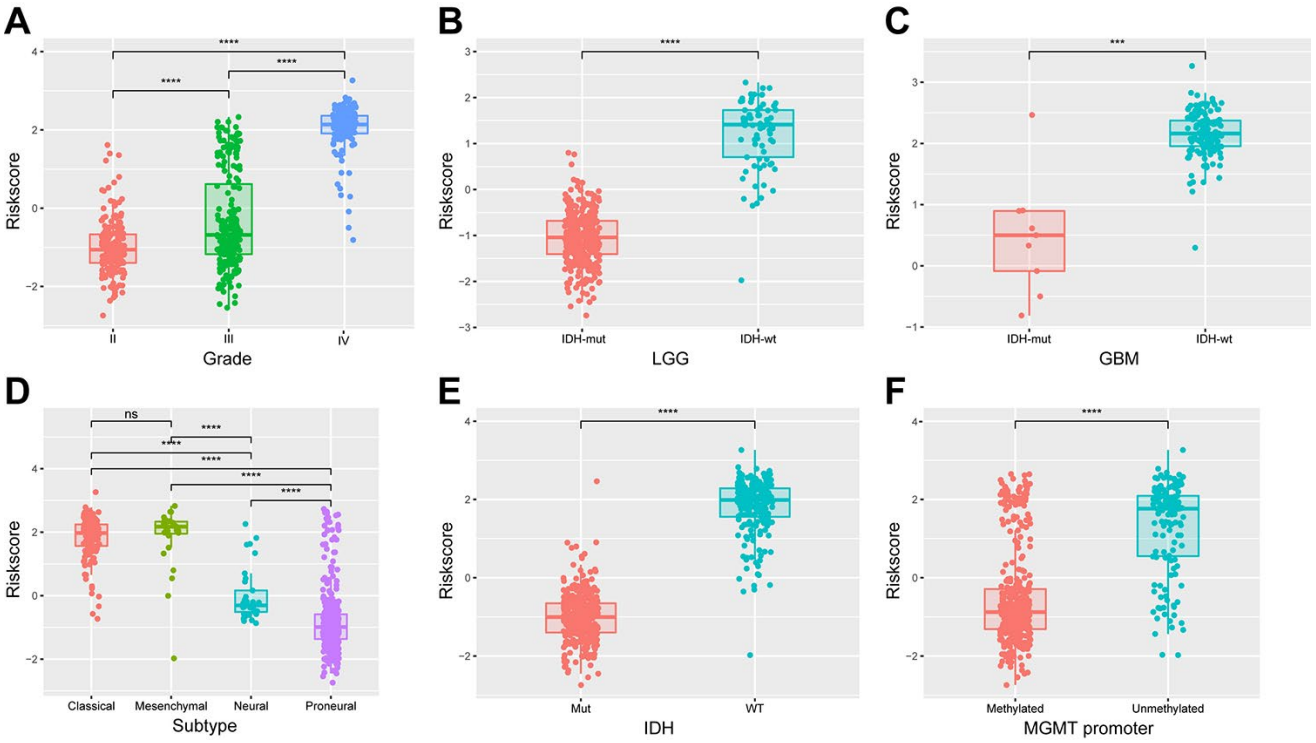

Figure 5. Association between the energy metabolism-related signature and pathologic features in TCGA cohort. (**A-F**) Distribution of the risk score in stratified patients by grade, subtype, IDH and MGMT promoter status.

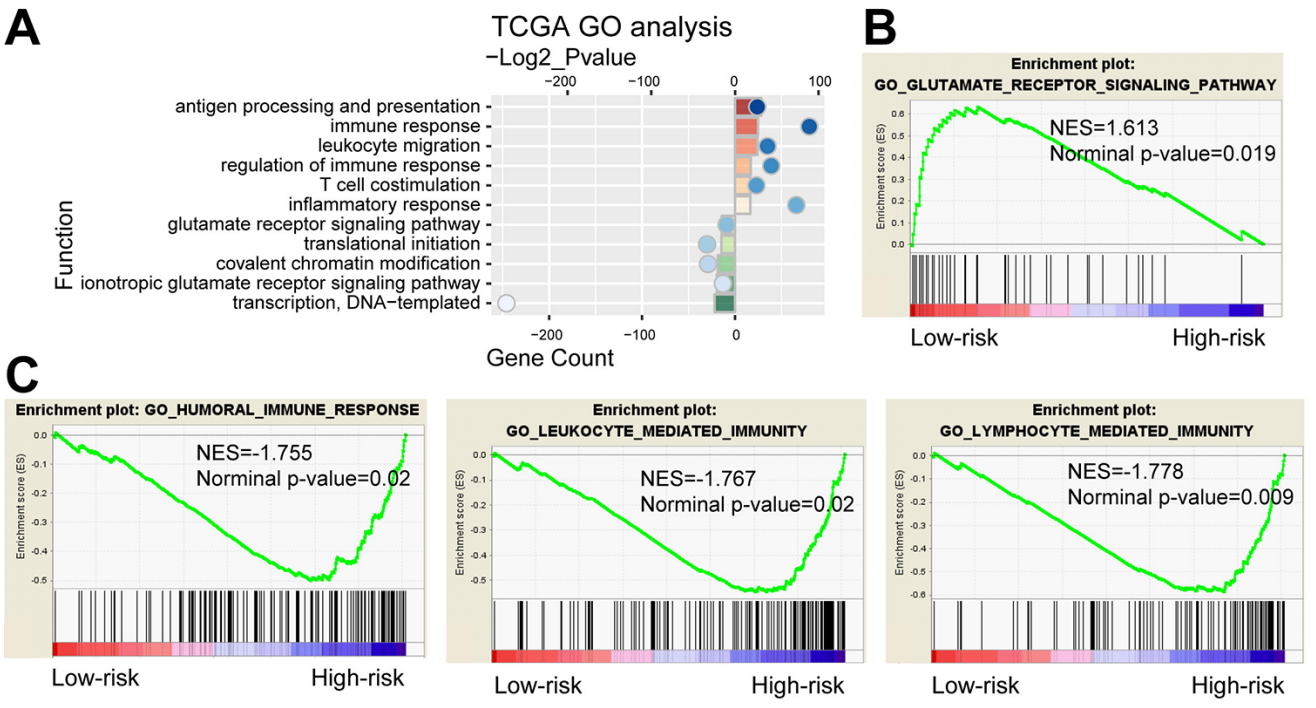

Figure 6. Functional analysis of the 29-gene signature. (**A**) GO annotations based on the top 2000 genes positively and negatively associated with the 29-gene signature. (**B-C**) GSEA analysis based on the median value of risk score.

Table 3. Characteristics of patients in low-risk and high-risk groups in TCGA cohort.

Characteristics	n	Risk score		*P*-value
		Low	High	
Total Cases	550	275	275	
Age				
≤48	287	197	90	**<0.001**
>48	263	78	185	
Gender				
Male	319	156	163	0.307
Female	231	119	112	
Subtype				
Classical	141	2	139	**<0.001**
Mesenchymal	31	1	30	
Proneural	345	264	81	
Neural	33	8	25	
Grade				
II	191	155	36	**<0.001**
III	211	119	92	
IV	148	1	147	
IDH				
Mut	338	274	64	**<0.001**
WT	212	1	211	
MGMT promoter				
Methylated	383	257	126	**<0.001**
Unmethylated	135	18	117	
NA	32	0	32	

IDH = isocitrate dehydrogenase;
MGMT = methylguanine methyltransferase.

and glutamate receptor signaling pathway (Figure 6A). GSEA found that the differentially expressed genes in two groups were associated with humoral immune response, leukocyte mediated immunity, lymphocyte mediated immunity and glutamate receptor signaling pathway (Figure 6B and C). As shown in Supplementary Figure 8, analysis of the CGGA cohort displayed consensus results. Moreover, we also performed functional analyses in LGG and GBM respectively. Consequently, GO and GESA analyses showed similar outcomes (Supplementary Figure 9). The corresponding biologic functions might contribute to patients' high risk and poor prognosis.

DISCUSSION

Increasing evidence has revealed that metabolism deregulation is one of the emerging hallmarks of cancer cells. Energy metabolic difference between normal and tumor cells has attracted extensive attention worldwide for decades. In glioma, resent studies demonstrated that multiple catabolic pathways are involved in its energy metabolism, such as glycolysis, OXPHOS and fatty acid metabolism [18]. In the present study, we detected the local energy metabolic status and its prognostic value in patients with glioma with RNA sequencing data. Since energy metabolic gene could distinguish patients' clinical and molecular features, we further developed a signature that could stratify patients with high or low-risk of poor outcome. Considering that univariate Cox model is insufficient for variables selection with dimensional data, we first performed univariate Cox model to filter genes related to OS and applied an elastic net regression Cox model to increase the predictive performance of the prognostic index [19], and the obtained 29 genes showed a cumulative effect on survival prediction. This energy metabolism-related signature could serve as a powerful prognostic indicator and stratify patients for energy metabolism-targeted therapies in future.

Functional analysis suggested that differences of biologic processes between high-risk and low-risk groups of patients were mainly involved in immune and inflammatory response, indicating an interface between energy metabolism and immune environment. Recently, compelling studies have identified numerous alterations in glioma cells metabolism that may play an important role in immune regulation [20]. The accumulation of lactic acid from aerobic glycolysis in tumor cells can shape the immune system, including increasing the transcription of cytokines, inhibiting differentiation of monocytes to dendritic cells [21, 22]. Expression of *IDO1* (indoleamine 2, 3-dioxygenase 1), tryptophan metabolic enzyme, increases the recruitment of regulatory T cells and negatively impacts survival in glioma cells [23]. *IDO1* inhibition combined with *PD-L1* and *CTLA-4* inhibitors can enhance the therapeutic efficacy [24]. M2 macrophages use arginine to produce ornithine and urea, leading to anti-inflammatory effects and CD4+ T cell-mediated immune suppression [25]. To further understand the relationship between this risk score and immune response, immune checkpoints (*PD-1*, *PD-L1*, *CTLA-4*, *CD80* and *TIM-3*) [26-28] and inflammatory genes (*INF-α*, *INF-γ*, *TNF-α*, *IL-6*, *IL-17*, *CCL2*, *CXCL2 and HLA-A*) [29-32] were selected. Correlation analysis revealed that expression of these immune checkpoints was positively correlated with the risk score in both TCGA and CGGA cohorts (Supplementary Figure 10A and B), indicating an

immunosuppressive state in high-risk group of glioma patients. In addition, the risk score was also positively associated with the expression of *INF-γ*, *IL-6*, *CCL2* and *HLA-A* (Supplementary Figure 10C and D), suggesting that macrophages and T cell mediated immune response were involved in high-risk group of glioma patients.

Collectively, we uncovered the energy metabolism gene expression and its prognostic value in diffuse glioma and identified an energy metabolism-related signature which could classify glioma patients with high-risk and low-risk groups of reduced survival. However, more prospective studies were further needed and the predictive ability of this signature should be tested for clinical application. Our findings offer new understanding about energy metabolism status and will benefit energy metabolism-targeted therapies in glioma.

MATERIALS AND METHODS

Datasets

The TCGA RNA sequencing data and corresponding clinical information, such as age, gender, histology, methylguanine methyltransferase (MGMT) promoter status, isocitrate dehydrogenase (IDH) mutation status and survival information, were downloaded from TCGA database (http://cancergemome.nih.gov/) as training set. Similarly, the CGGA RNA sequencing data and clinical information ware downloaded from CGGA database (http://www.cgga.org.cn) as validation set [33]. The characteristics of glioma patients from these two datasets were listed in Table 4.

Table 4. Clinical characteristics of diffuse glioma patients.

TCGA cohort (550)		CGGA cohort (309)	
Characteristic	**No.**	**Characteristic**	**No.**
Age		**Age**	
≤48	287	≤43	166
>48	263	>43	143
Gender		**Gender**	
Male	319	Male	194
Female	231	Female	115
Subtype		**Subtype**	
Classical	141	Classical	69
Mesenchymal	31	Mesenchymal	65
Proneural	345	Proneural	99
Neural	33	Neural	76
Grade		**Grade**	
II	191	II	104
III	211	III	67
IV	148	IV	138
IDH		**IDH**	
Mut	338	Mut	155
WT	212	WT	154
MGMT promoter		**MGMT promoter**	
Methylated	383	Methylated	136
Unmethylated	135	Unmethylated	111
NA	32	NA	62

IDH = isocitrate dehydrogenase; MGMT = methylguanine methyltransferase.

Consensus clustering

Two energy metabolism-related gene sets (Reactome energy metabolism and energy-requiring part of metabolism) were downloaded from Molecular Signature Database v5.1 (MSigDB) (http://www.broad.mit.edu/gsea/msigdb/) [34]. Overlapped genes were removed and the acquired energy metabolism-related gene set contained 587 genes. Measured by median absolute deviation (MAD), the most variable genes were used for subsequent clustering. Consensus clustering was performed with R package "ConsensusClusterPlus". The optimal number of subgroups was evaluated using cumulative distribution function (CDF) and consensus matrices [35].

Gene signature identification

Significance analysis of microarray (SAM) was performed to identify the differentially expressed energy metabolism-related genes between lower grade glioma (LGG) and GBM with R package "samr". Simultaneously, univariate Cox analysis was used to determine the prognosis-related genes. After that, the Cox proportional hazards model was applied for selection of optimal prognostic gene set with R package "glmnet", which was suitable for the regression analysis of high-dimensional data [19]. Risk score for each patient of the TCGA training set was calculated with the linear combinational of the signature gene expression weighted by their regression coefficients. Risk score = ($expr_{gene1}$ x $coefficient_{gene1}$) + ($expr_{gene2}$ x $coefficient_{gene2}$) + … + ($expr_{genen}$ x $coefficient_{genen}$). Then, the regression coefficients from the training set was applied into the CGGA validation set for risk score calculation.

Gene ontology (GO), gene set enrichment analysis (GSEA) and principal components analysis (PCA)

GO analysis was applied for the main function annotation of differential expression genes (http://david.ncifcrf.gov/). GSEA was performed to identify gene sets of statistical difference between two groups by using the GSEA v3 software (http://www.broadinstitute.org/gsea/index.jsp) [34]. PCA was carried out to detect expression difference within groups using R package "princomp" [36].

Statistical analysis

According to the risk score, patients were divided into high-risk and low-risk groups based on the median value. Kaplan-Meier with 2-sided log-rank test was used to evaluate the overall survival (OS) differences between these two groups. Chi-square test was performed to detect the difference of the pathologic features between these two groups of patients. Univariate and multivariate Cox regression analysis was conducted to identify independent prognostic factors. ROC curve analysis was used to predict OS with R package "pROC". All statistical analyses were conducted using SPSS or R software. $P<0.05$ was considered significant.

Abbreviations

CGGA, Chinese Glioma Genome Atlas; TCGA, The Cancer Genome Atlas; OS, overall survival; LGG, lower grade glioma; GBM, glioblastoma; HR, hazard ratio; CI, confidence interval; GO, gene ontology; GSEA, gene set enrichment analysis; OXPHOS, oxidative phosphorylation; TCA, tricarboxylic acid; AUC, area under the curve; PCA, principal components analysis.

AUTHOR CONTRIBUTIONS

Fan Wu designed the study and wrote the manuscript. Zhengui Zhou, Ruoyu Huang and Ruichao Chai performed the gene analysis. Xiaohong Zhou, Zhiping Hu, Wenbiao Wang, Baoguo Chen, Lintao Deng and Yuqing Liu collected the clinical data.

ACKNOWLEDGMENT

The authors accomplishing this work represent the Chinese Glioma Cooperative Group (CGCG).

CONFLICTS OF INTEREST

The authors have no conflict of interest.

FUNDING

National Natural Science Foundation of China (NSFC)/Research Grants Council (RGC) Joint Research Scheme (81761168038); The National Key Research and Development Plan (2016YFC0902500); National Natural Science Foundation of China (81672479, 81773208).

REFERENCES

1. Fumarola C, Petronini PG, Alfieri R. Impairing energy metabolism in solid tumors through agents targeting oncogenic signaling pathways. Biochem Pharmacol. 2018; 151:114–25. https://doi.org/10.1016/j.bcp.2018.03.006

2. Warburg O. The metabolism of carcinoma cells. J Cancer Res. 1925; 9:148–63. https://doi.org/10.1158/jcr.1925.148

3. Sonveaux P, Végran F, Schroeder T, Wergin MC, Verrax J, Rabbani ZN, De Saedeleer CJ, Kennedy KM, Diepart C, Jordan BF, Kelley MJ, Gallez B, Wahl ML, et al. Targeting lactate-fueled respiration selectively kills hypoxic tumor cells in mice. J Clin Invest. 2008; 118:3930–42. https://doi.org/10.1172/JCI36843

4. Whitaker-Menezes D, Martinez-Outschoorn UE, Flomenberg N, Birbe RC, Witkiewicz AK, Howell A, Pavlides S, Tsirigos A, Ertel A, Pestell RG, Broda P, Minetti C, Lisanti MP, Sotgia F. Hyperactivation of oxidative mitochondrial metabolism in epithelial cancer cells in situ: visualizing the therapeutic effects of metformin in tumor tissue. Cell Cycle. 2011; 10:4047–64. https://doi.org/10.4161/cc.10.23.18151

5. Faubert B, Li KY, Cai L, Hensley CT, Kim J, Zacharias LG, Yang C, Do QN, Doucette S, Burguete D, Li H, Huet G, Yuan Q, et al. Lactate metabolism in human lung tumors. Cell. 2017; 171:358–371.e9. https://doi.org/10.1016/j.cell.2017.09.019

6. Nieman KM, Kenny HA, Penicka CV, Ladanyi A, Buell-Gutbrod R, Zillhardt MR, Romero IL, Carey MS, Mills GB, Hotamisligil GS, Yamada SD, Peter ME, Gwin K, Lengyel E. Adipocytes promote ovarian cancer metastasis and provide energy for rapid tumor growth. Nat Med. 2011; 17:1498–503. https://doi.org/10.1038/nm.2492

7. Bonuccelli G, Tsirigos A, Whitaker-Menezes D, Pavlides S, Pestell RG, Chiavarina B, Frank PG, Flomenberg N, Howell A, Martinez-Outschoorn UE, Sotgia F, Lisanti MP. Ketones and lactate "fuel" tumor growth and metastasis: evidence that epithelial cancer cells use oxidative mitochondrial metabolism. Cell Cycle. 2010; 9:3506–14.

https://doi.org/10.4161/cc.9.17.12731

8. Le A, Lane AN, Hamaker M, Bose S, Gouw A, Barbi J, Tsukamoto T, Rojas CJ, Slusher BS, Zhang H, Zimmerman LJ, Liebler DC, Slebos RJ, et al. Glucose-independent glutamine metabolism via TCA cycling for proliferation and survival in B cells. Cell Metab. 2012; 15:110–21. https://doi.org/10.1016/j.cmet.2011.12.009

9. Fan J, Kamphorst JJ, Mathew R, Chung MK, White E, Shlomi T, Rabinowitz JD. Glutamine-driven oxidative phosphorylation is a major ATP source in transformed mammalian cells in both normoxia and hypoxia. Mol Syst Biol. 2013; 9:712. https://doi.org/10.1038/msb.2013.65

10. Wen PY, Kesari S. Malignant gliomas in adults. N Engl J Med. 2008; 359:492–507. https://doi.org/10.1056/NEJMra0708126

11. Phillips HS, Kharbanda S, Chen R, Forrest WF, Soriano RH, Wu TD, Misra A, Nigro JM, Colman H, Soroceanu L, Williams PM, Modrusan Z, Feuerstein BG, Aldape K. Molecular subclasses of high-grade glioma predict prognosis, delineate a pattern of disease progression, and resemble stages in neurogenesis. Cancer Cell. 2006; 9:157–73. https://doi.org/10.1016/j.ccr.2006.02.019

12. Brennan CW, Verhaak RG, McKenna A, Campos B, Noushmehr H, Salama SR, Zheng S, Chakravarty D, Sanborn JZ, Berman SH, Beroukhim R, Bernard B, Wu CJ, et al, and TCGA Research Network. The somatic genomic landscape of glioblastoma. Cell. 2013; 155:462–77. https://doi.org/10.1016/j.cell.2013.09.034

13. Osuka S, Van Meir EG. Overcoming therapeutic resistance in glioblastoma: the way forward. J Clin Invest. 2017; 127:415–26. https://doi.org/10.1172/JCI89587

14. Khurshed M, Molenaar RJ, Lenting K, Leenders WP, van Noorden CJ. In silico gene expression analysis reveals glycolysis and acetate anaplerosis in IDH1 wild-type glioma and lactate and glutamate anaplerosis in IDH1-mutated glioma. Oncotarget. 2017; 8:49165–77. https://doi.org/10.18632/oncotarget.17106

15. Lin H, Patel S, Affleck VS, Wilson I, Turnbull DM, Joshi AR, Maxwell R, Stoll EA. Fatty acid oxidation is required for the respiration and proliferation of malignant glioma cells. Neuro-oncol. 2017; 19:43–54. https://doi.org/10.1093/neuonc/now128

16. Vlashi E, Lagadec C, Vergnes L, Matsutani T, Masui K, Poulou M, Popescu R, Della Donna L, Evers P, Dekmezian C, Reue K, Christofk H, Mischel PS, Pajonk F. Metabolic state of glioma stem cells and nontumorigenic cells. Proc Natl Acad Sci USA. 2011; 108:16062–67. https://doi.org/10.1073/pnas.1106704108

17. Grube S, Göttig T, Freitag D, Ewald C, Kalff R, Walter J. Selection of suitable reference genes for expression analysis in human glioma using RT-qPCR. J Neurooncol. 2015; 123:35–42. https://doi.org/10.1007/s11060-015-1772-7

18. Strickland M, Stoll EA. Metabolic Reprogramming in Glioma. Front Cell Dev Biol. 2017; 5:43. https://doi.org/10.3389/fcell.2017.00043

19. Hughey JJ, Butte AJ. Robust meta-analysis of gene expression using the elastic net. Nucleic Acids Res. 2015; 43:e79. https://doi.org/10.1093/nar/gkv229

20. Chinnaiyan P, Kensicki E, Bloom G, Prabhu A, Sarcar B, Kahali S, Eschrich S, Qu X, Forsyth P, Gillies R. The metabolomic signature of malignant glioma reflects accelerated anabolic metabolism. Cancer Res. 2012; 72:5878–88. https://doi.org/10.1158/0008-5472.CAN-12-1572-T

21. Ghesquière B, Wong BW, Kuchnio A, Carmeliet P. Metabolism of stromal and immune cells in health and disease. Nature. 2014; 511:167–76. https://doi.org/10.1038/nature13312

22. Becker JC, Andersen MH, Schrama D, Thor Straten P. Immune-suppressive properties of the tumor microenvironment. Cancer Immunol Immunother. 2013; 62:1137–48. https://doi.org/10.1007/s00262-013-1434-6

23. Wainwright DA, Balyasnikova IV, Chang AL, Ahmed AU, Moon KS, Auffinger B, Tobias AL, Han Y, Lesniak MS. IDO expression in brain tumors increases the recruitment of regulatory T cells and negatively impacts survival. Clin Cancer Res. 2012; 18:6110–21. https://doi.org/10.1158/1078-0432.CCR-12-2130

24. Wainwright DA, Chang AL, Dey M, Balyasnikova IV, Kim CK, Tobias A, Cheng Y, Kim JW, Qiao J, Zhang L, Han Y, Lesniak MS. Durable therapeutic efficacy utilizing combinatorial blockade against IDO, CTLA-4, and PD-L1 in mice with brain tumors. Clin Cancer Res. 2014; 20:5290–301. https://doi.org/10.1158/1078-0432.CCR-14-0514

25. Rath M, Müller I, Kropf P, Closs EI, Munder M. Metabolism via arginase or nitric oxide synthase: two competing arginine pathways in macrophages. Front Immunol. 2014; 5:532. https://doi.org/10.3389/fimmu.2014.00532

26. Berghoff AS, Kiesel B, Widhalm G, Rajky O, Ricken G, Wöhrer A, Dieckmann K, Filipits M, Brandstetter A,

Weller M, Kurscheid S, Hegi ME, Zielinski CC, et al. Programmed death ligand 1 expression and tumor-infiltrating lymphocytes in glioblastoma. Neuro-oncol. 2015; 17:1064–75. https://doi.org/10.1093/neuonc/nou307

27. Preusser M, Lim M, Hafler DA, Reardon DA, Sampson JH. Prospects of immune checkpoint modulators in the treatment of glioblastoma. Nat Rev Neurol. 2015; 11:504–14. https://doi.org/10.1038/nrneurol.2015.139

28. Li G, Wang Z, Zhang C, Liu X, Cai J, Wang Z, Hu H, Wu F, Bao Z, Liu Y, Zhao L, Liang T, Yang F, et al. Molecular and clinical characterization of TIM-3 in glioma through 1,024 samples. OncoImmunology. 2017; 6:e1328339. https://doi.org/10.1080/2162402X.2017.1328339

29. Guthrie GJ, Roxburgh CS, Horgan PG, McMillan DC. Does interleukin-6 link explain the link between tumour necrosis, local and systemic inflammatory responses and outcome in patients with colorectal cancer? Cancer Treat Rev. 2013; 39:89–96. https://doi.org/10.1016/j.ctrv.2012.07.003

30. Germano G, Allavena P, Mantovani A. Cytokines as a key component of cancer-related inflammation. Cytokine. 2008; 43:374–79. https://doi.org/10.1016/j.cyto.2008.07.014

31. Corrales L, Gajewski TF. Molecular pathways: targeting the stimulator of interferon genes (STING) in the immunotherapy of cancer. Clin Cancer Res. 2015; 21:4774–79. https://doi.org/10.1158/1078-0432.CCR-15-1362

32. Kolls JK, Lindén A. Interleukin-17 family members and inflammation. Immunity. 2004; 21:467–76. https://doi.org/10.1016/j.immuni.2004.08.018

33. Yan W, Zhang W, You G, Zhang J, Han L, Bao Z, Wang Y, Liu Y, Jiang C, Kang C, You Y, Jiang T. Molecular classification of gliomas based on whole genome gene expression: a systematic report of 225 samples from the Chinese Glioma Cooperative Group. Neuro-oncol. 2012; 14:1432–40. https://doi.org/10.1093/neuonc/nos263

34. Subramanian A, Tamayo P, Mootha VK, Mukherjee S, Ebert BL, Gillette MA, Paulovich A, Pomeroy SL, Golub TR, Lander ES, Mesirov JP. Gene set enrichment analysis: a knowledge-based approach for interpreting genome-wide expression profiles. Proc Natl Acad Sci USA. 2005; 102:15545–50. https://doi.org/10.1073/pnas.0506580102

35. Li R, Qian J, Wang YY, Zhang JX, You YP. Long noncoding RNA profiles reveal three molecular subtypes in glioma. CNS Neurosci Ther. 2014; 20:339–43. https://doi.org/10.1111/cns.12220

36. Cheng W, Ren X, Zhang C, Cai J, Liu Y, Han S, Wu A. Bioinformatic profiling identifies an immune-related risk signature for glioblastoma. Neurology. 2016; 86:2226–34. https://doi.org/10.1212/WNL.0000000000002770

SUPPLEMENTARY MATERIAL

Supplementary Table 1. Characteristics of patients in class 1 and class 2 in CGGA cohort.

Characteristics	n	Class 1	Class 2	*P*-value
Total Cases	309	185	124	
Age				
≤43	166	80	86	**<0.001**
>43	143	105	38	
Gender				
Male	194	120	74	0.401
Female	115	65	50	
Subtype				
Classical	69	64	5	**<0.001**
Mesenchymal	65	65	0	
Proneural	99	44	55	
Neural	76	12	64	
Grade				
II	104	17	87	**<0.001**
III	67	41	26	
IV	138	127	11	
IDH				
Mut	155	51	104	**<0.001**
WT	154	134	20	
MGMT promoter				
Methylated	136	79	57	**<0.001**
Unmethylated	111	81	30	
NA	62	25	37	

IDH = isocitrate dehydrogenase; MGMT = methylguanine methyltransferase.

Supplementary Table 2. Univariate and multivariate Cox regression analysis of clinical pathologic features for OS in CGGA cohort.

Characteristics	Univariate analysis			Multivariate analysis		
	HR	95% CI	*P*-value	HR	95% CI	*P*-value
Age	1.038	1.022-1.053	**<0.001**	0.999	0.983-1.016	0.914
Gender	0.843	0.597-1.189	0.33			
Grade	3.469	2.709-4.443	**<0.001**	2.097	1.511-2.91	**<0.001**
Subtype	0.583	0.492-0.691	**<0.001**	0.782	0.659-0.929	0.005
IDH	0.257	0.179-0.37	**<0.001**	1.106	0.566-2.159	0.768
MGMT Promoter	0.529	0.374-0.75	**<0.001**	0.78	0.53-1.147	0.207
Risk score	2.232	1.912-2.607	**<0.001**	1.556	1.161-2.086	**0.003**

HR = hazard ratio; CI = confidence interval; IDH = isocitrate dehydrogenase; MGMT = methylguanine methyltransferase.

Supplementary Table 3. Characteristics of patients in low-risk and high-risk groups in CGGA cohort.

Characteristics	n	Risk score		*P*-value
		Low	High	
Total Cases	309	154	155	
Age				
≤43	166	112	54	**<0.001**
>43	143	42	101	
Gender				
Male	194	91	103	0.181
Female	115	63	52	
Subtype				
Classical	69	8	61	**<0.001**
Mesenchymal	65	3	62	
Proneural	99	86	13	
Neural	76	57	19	
Grade				
II	104	92	12	**<0.001**
III	67	36	31	
IV	138	26	112	
IDH				
Mut	155	136	19	**<0.001**
WT	154	18	136	
MGMT promoter				
Methylated	136	79	57	**<0.001**
Unmethylated	111	30	81	
NA	62	45	17	

IDH = isocitrate dehydrogenase; MGMT = methylguanine methyltransferase.

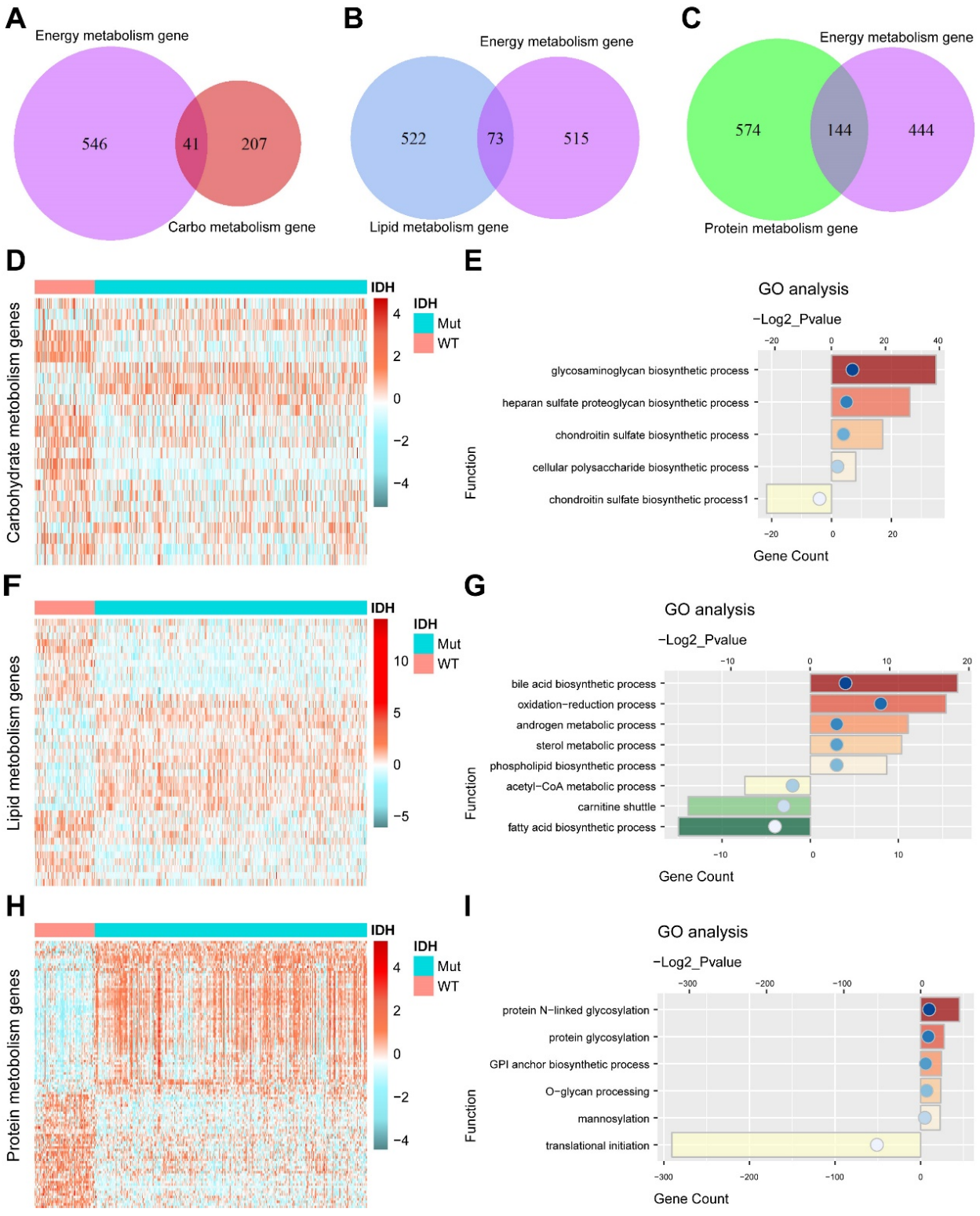

Supplementary Figure 1. Profile of carbohydrate, lipid and protein metabolism genes involved in energy metabolism between IDH-wt and IDH-mut LGG. (**A-C**) Venn diagrams show carbohydrate, lipid and protein metabolism genes involved in energy metabolism. (**D** and **E**) Heat map and GO analysis of differentially expressed carbohydrate metabolism genes between IDH-wt and IDH-mut LGG. (**F** and **G**) Heat map and GO analysis of differentially expressed lipid metabolism genes. (H and I) Heat map and GO analysis of differentially expressed protein metabolism genes.

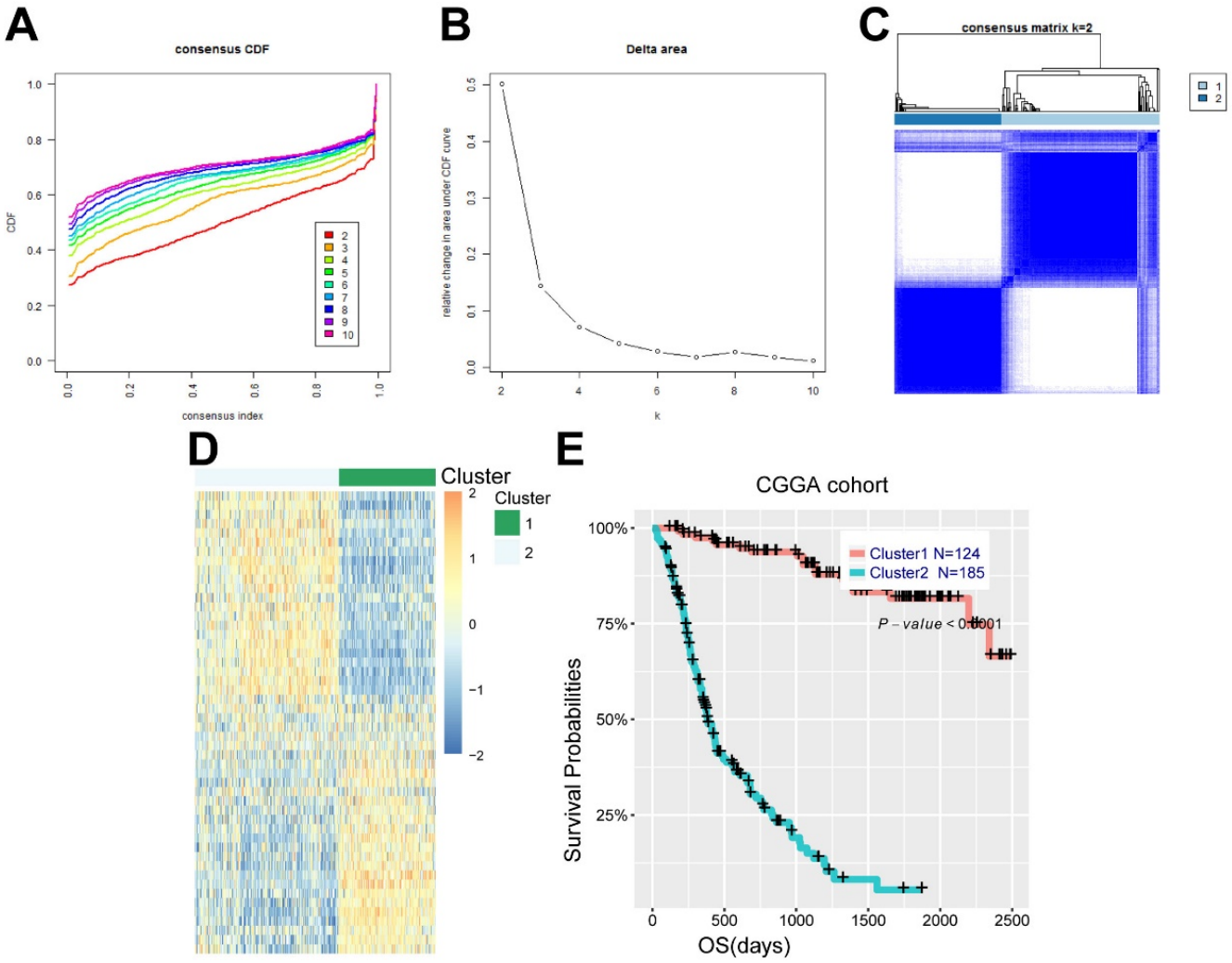

Supplementary Figure 2. Energy metabolism-related genes could distinguish glioma patients with different clinical and molecular features. (**A**) Consensus clustering CDF for k = 2 to k = 10. (**B**) Relative change in area under CDF curve for k = 2 to k = 10. (**C**) Consensus clustering matrix of 309 samples from CGGA dataset for k = 2. (**D**) Heat map of two clusters defined by the top 50 variable expression genes. (**E**) survival analysis of patients in cluster 1 and cluster 2.

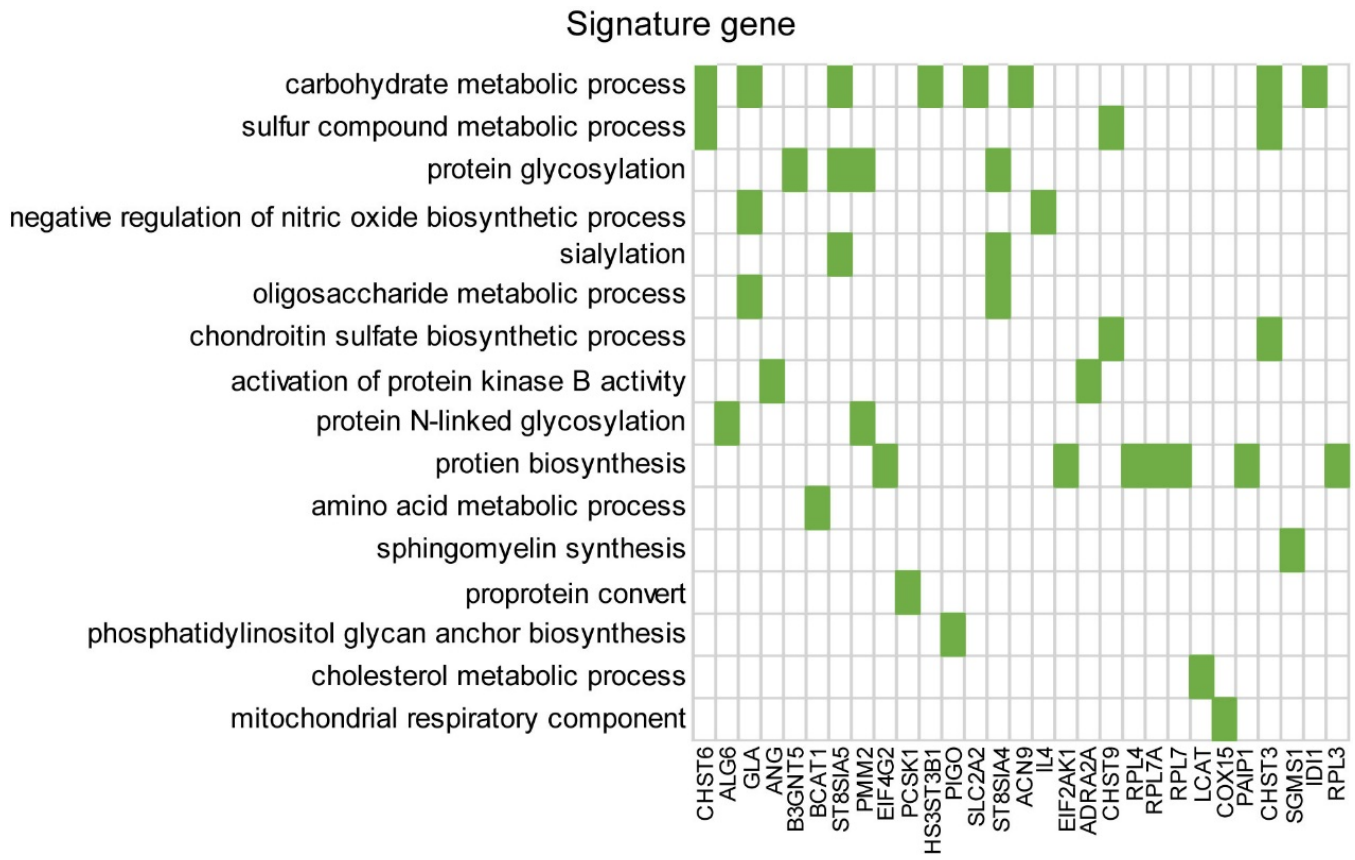

Supplementary Figure 3. Functional annotation of the signature genes.

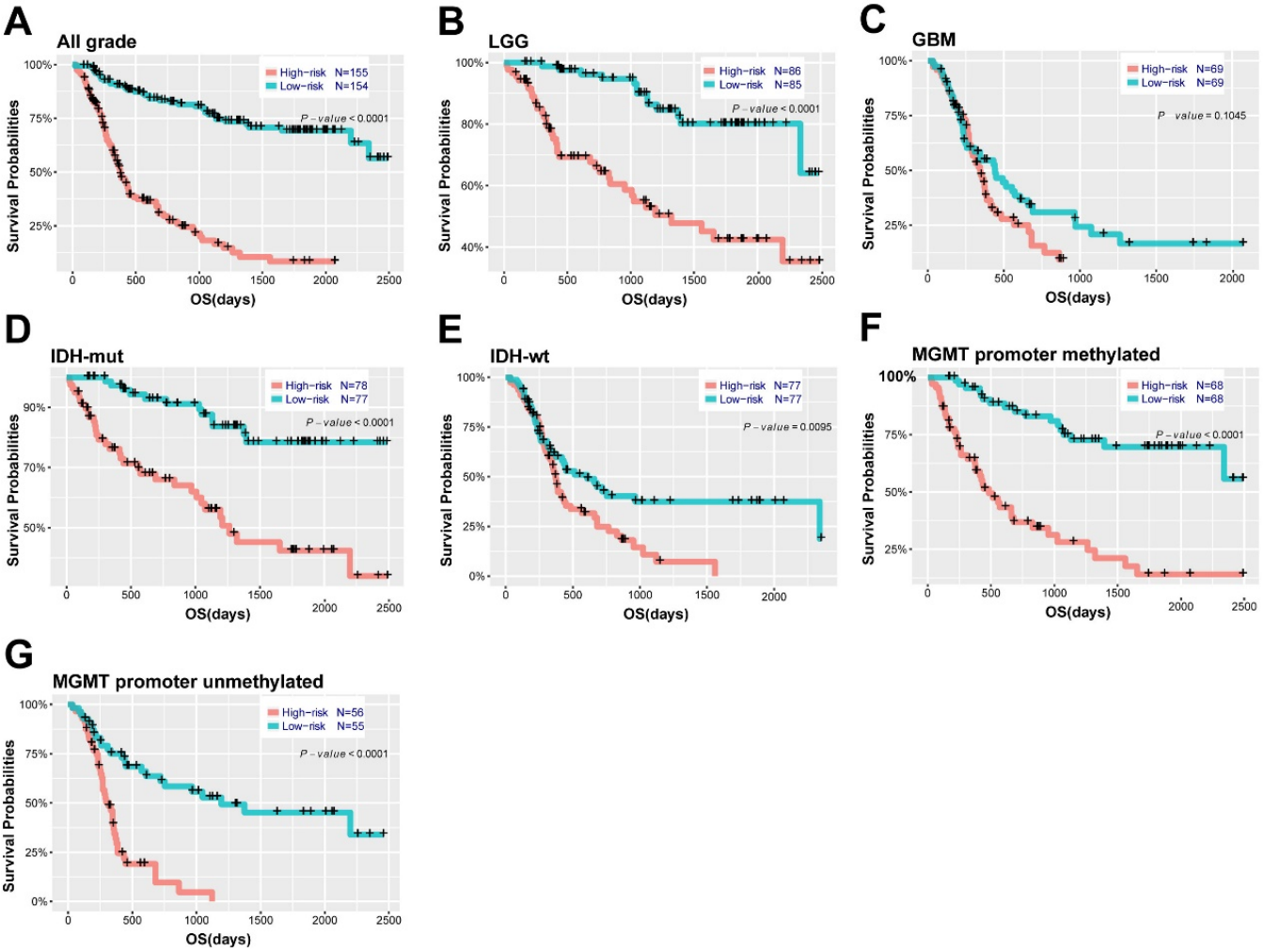

Supplementary Figure 4. Prognostic evaluation of the 29-gene signature in stratified patients of CGGA cohort. (**A-G**) Survival analysis of the signature in patients stratified by grade, IDH and MGMT promoter status.

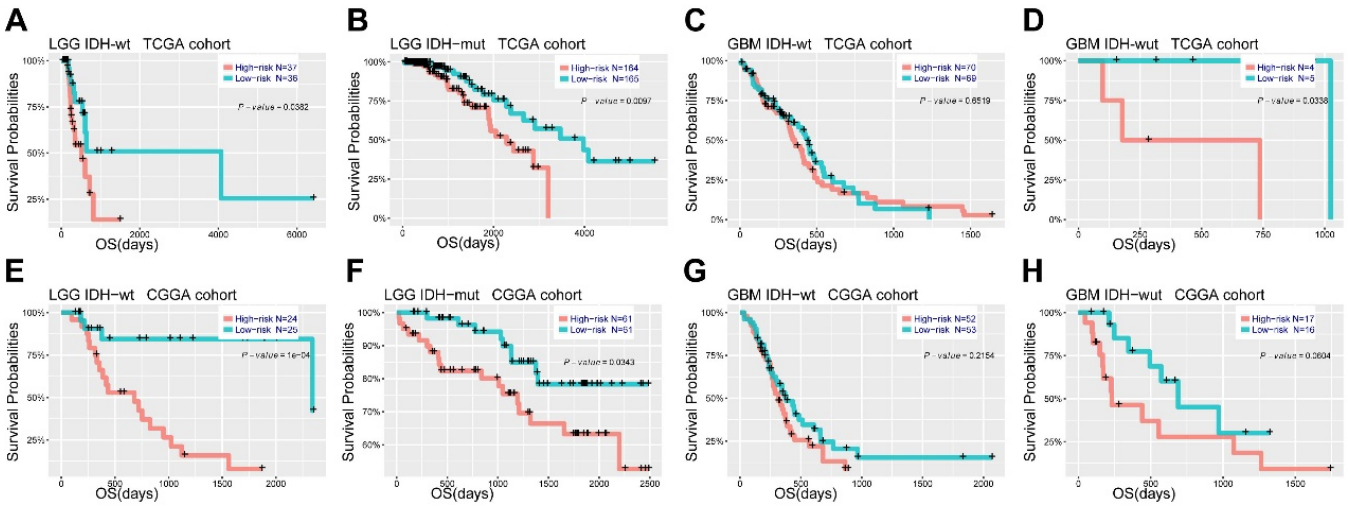

Supplementary Figure 5. Prognostic evaluation of the 29-gene signature in molecular subgroups. (**A-D**) Survival analysis of the signature in LGG IDH-wt, LGG IDH-mut, GBM IDH-wt and GBM IDH-mut patients of TCGA cohort. (**E-H**) Survival analysis of the signature in LGG IDH-wt, LGG IDH-mut, GBM IDH-wt and GBM IDH-mut patients of CGGA cohort.

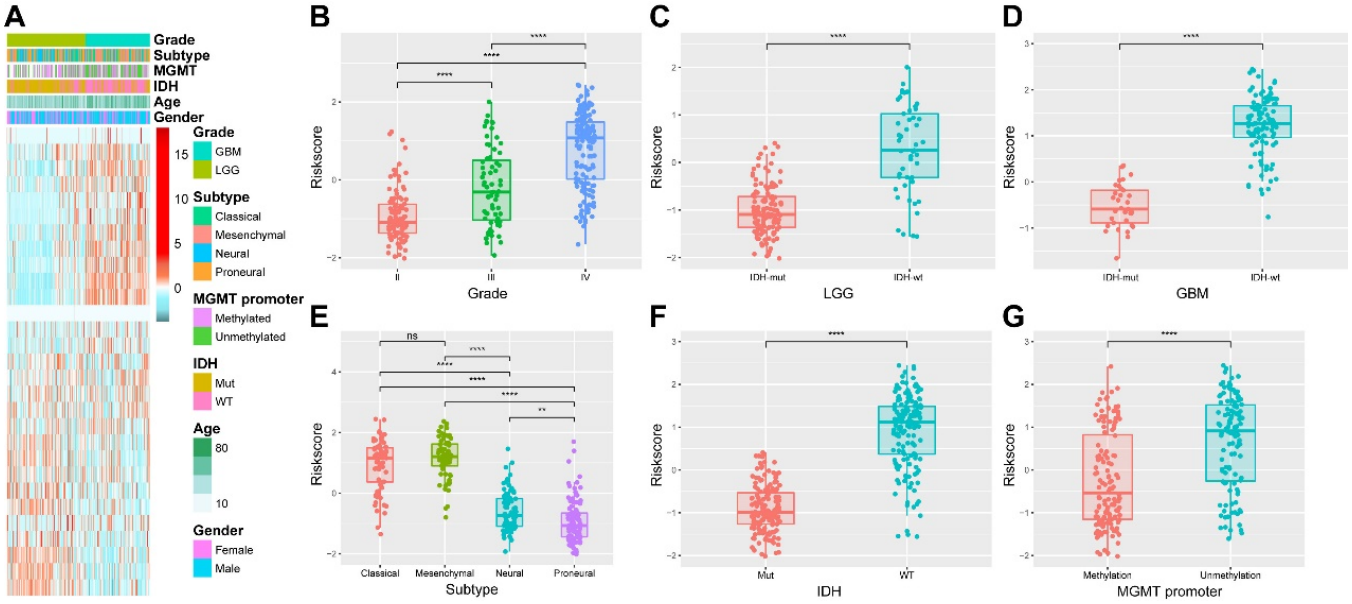

Supplementary Figure 6. Association between the energy metabolism-related signature and clinical features in CGGA cohort. (**A**) Heatmap of the 29 genes of the signature based on the risk score value. (**B-G**) Distribution of the risk score in stratified patients by grade, subtype, IDH and MGMT promoter status.

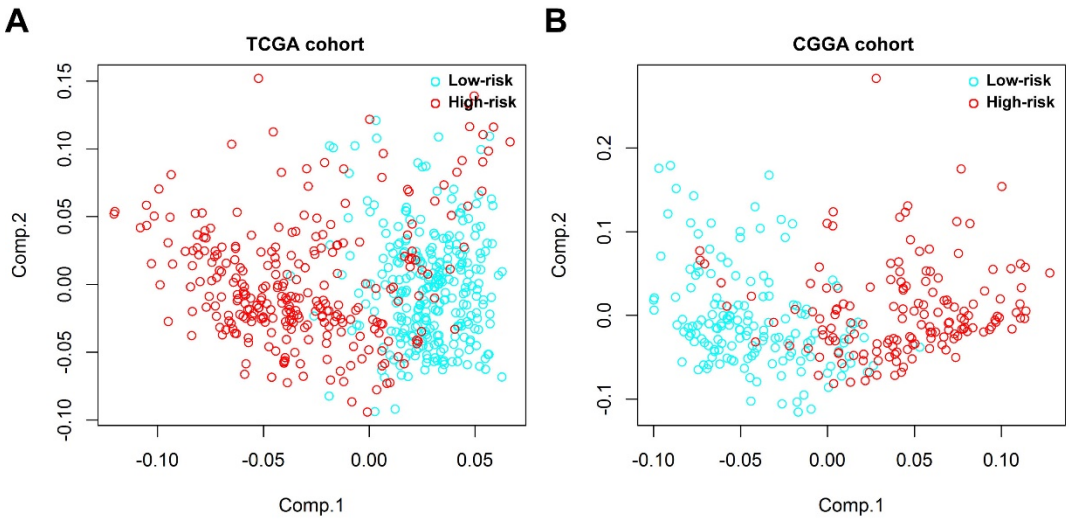

Supplementary Figure 7. Principal components analysis of high and low-risk groups of patients based on whole gene expression data. (**A**-**B**) PCA in TCGA and CGGA cohorts.

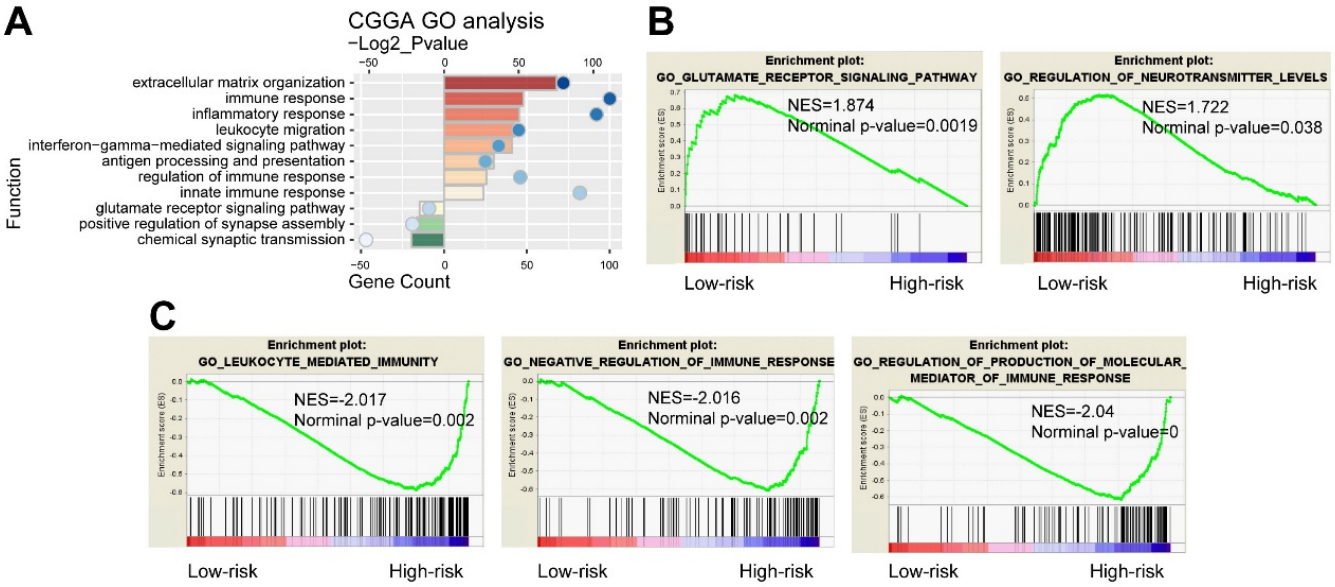

Supplementary Figure 8. Functional analysis of the 29-gene signature in CGGA cohort. (**A**) GO annotations based on the top 2000 genes positively and negatively associated with the 29-gene signature. (**B-C**) GSEA analysis based on the median value of risk score.

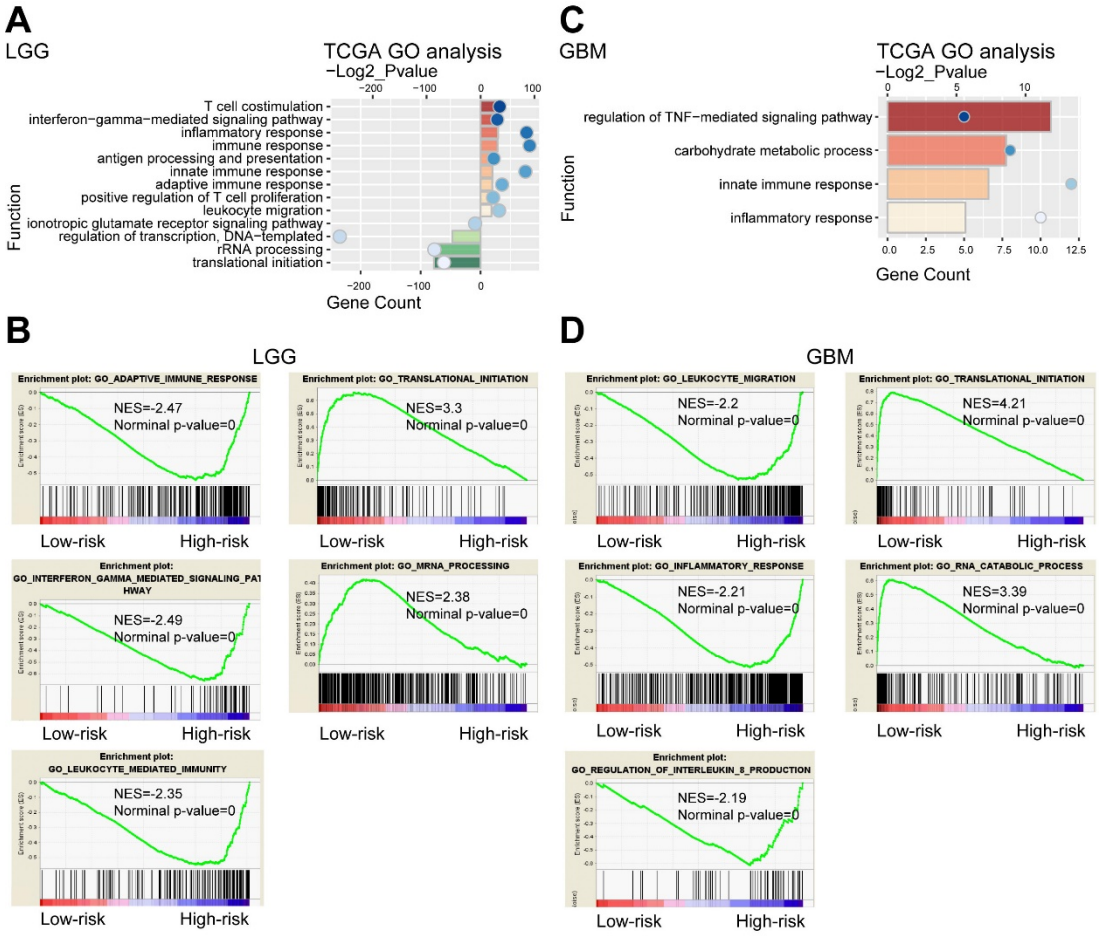

Supplementary Figure 9. Functional analysis of the 29-gene signature in LGG and GBM of TCGA cohort. (**A**) GO annotations based on the top 2000 genes positively and negatively associated with the 29-gene signature in LGG. (**B**) GSEA analysis based on the median value of risk score in LGG. (**C**) GO annotations based on the top 2000 genes positively and negatively associated with the 29-gene signature in GBM. (**D**) GSEA analysis based on the median value of risk score in GBM.

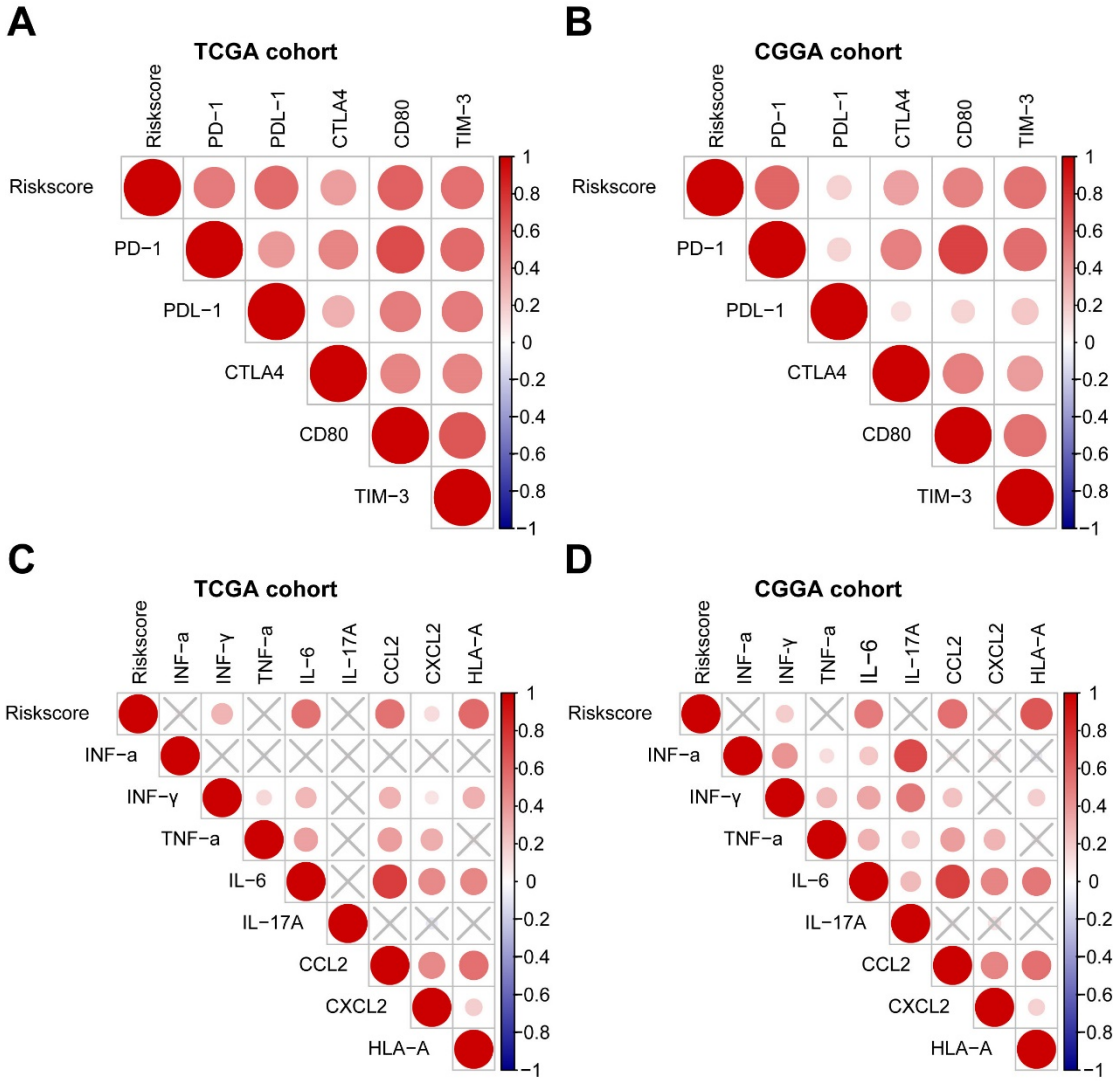

Supplementary Figure 10. Association between the energy metabolism-related signature and immune, inflammatory responses. (**A-B**) Correlation analysis between risk score and immune checkpoints. (**C-D**) Correlation analysis between risk score and inflammatory genes.